GMR
The Original

ANTI-INFLAMMATORY ACTIVITY OF SUSTAINABLE POLYMERIC ELECTROSPUN NANOSCAFFOLDS LOADED WITH GREEN SYNTHESIZED CuO NANOPARTICLES FROM *Chondracanthus exasperatus* EXTRACT

Sriranjani Dharmaprakash[1], Swetha P[2], Alagendran Subbarayalu[3]

[1]Saveetha Medical College & Hospital (SMCH), Saveetha Institute of Medical and Technical Sciences (SIMATS), Thandalam, Chennai, Tamil Nadu 602105, India. dsri12093@gmail.com.
[2]Department of Pathology, Saveetha Medical College and Hospital, Saveetha Institute of Medical And Technical Sciences (SIMATS), Thandalam, Chennai-602105, Tamil Nadu, India. Email: spswethu@gmail.com; ORCID: https://orcid.org/0009-0008-5190-5113.
[3]Clinical Neuroscience and Phytomedicine Laboratory, Department of Research, Saveetha College of Nursing (SCON), Saveetha Institute of Medical and Technical Sciences (SIMATS), Chennai 602105, Tamil Nadu, India. Email: proteinblg@gmail.com; alagendrans.scon@saveetha.com. ORCID: https://orcid.org/0009-0009-0749-7180.
*Correspondence: proteinblg@gmail.com; alagendrans.scon@saveetha.com (A.S.)

ABSTRACT
This study reports the fabrication of biocompatible starch/polyvinyl alcohol (PVA) electrospun nanoscaffolds embedded with copper oxide nanoparticles (CuO NPs) synthesized via an eco-friendly ultrasonic-assisted method using marine macroalgae *Chondracanthus exasperatus* extract. The green synthesis yielded uniformly dispersed, stable CuO NPs characterized by UV–Vis, Fourier Transform Infrared Spectroscopy (FTIR), X-ray diffraction (XRD), Scanning electron microscopy (SEM), and thermal analyses, confirming their crystalline nature, nanoparticle-polymer interaction, and enhanced thermal stability within the scaffold matrix. Morphological evaluation revealed bead-free, porous nanofibers with well-integrated nanoparticles conducive to biomedical applications. Dynamic light scattering (DLS) and zeta potential measurements demonstrated colloidal stability and moderate size uniformity of CuO nanoparticles. Importantly, the nanoscaffolds exhibited significant anti-inflammatory activity *in vitro*, outperforming both the algal extract and isolated nanoparticles, as evidenced by protein denaturation and xanthine oxidase inhibition assays, with efficacy comparable to diclofenac sodium. These findings highlight the potential of starch/PVA-CuO nanocomposites as sustainable, effective anti-inflammatory biomaterials for therapeutic applications.

KEYWORDS: *Chondracanthus exasperatus*, Green synthesis, CuO nanoparticles, starch/PVA nanoscaffolds, Anti-inflammatory activity.

1. INTRODUCTION

The increasing incidence of chronic inflammation-related conditions, including autoimmune diseases, arthritis, and various metabolic syndromes, has intensified the need for novel biomaterials with potent therapeutic activity and minimal side effects [1]. Traditional pharmaceutical agents such as non-steroidal anti-inflammatory drugs (NSAIDs) often present adverse gastrointestinal or renal effects, making them less suitable for long-term use [2]. As a result, there is growing interest in the development of biocompatible, biodegradable, and functionally active materials that can be tailored for therapeutic applications, especially in wound healing and tissue engineering [3]. In this context, the use of nanotechnology and natural bioactive compounds presents a promising interdisciplinary strategy for the design of multifunctional scaffolds with both structural and therapeutic potential [4].

Electrospinning has emerged as a versatile and cost-effective technique for fabricating nanofibrous scaffolds that closely mimic the extracellular matrix (ECM) of native tissues [5]. These fibrous constructs offer high surface-area-to-volume ratios, tunable porosity, and favorable mechanical properties—making them ideal for use in regenerative medicine, drug delivery, and biomedical device engineering [6]. However, the choice of polymeric materials for scaffold fabrication significantly influences their biocompatibility, degradability, and functional performance [7]. Natural polymers such as starch, when blended with synthetic polymers like polyvinyl alcohol (PVA), enhance not only the bioactivity but also the processability and mechanical integrity of electrospun fibers

[8]. Starch, being biodegradable and non-toxic, improves the hydrophilicity and cell adhesion properties of the resulting scaffold, whereas PVA contributes to fiber uniformity and tensile strength during electrospinning [9].

Incorporating bioactive nanoparticles into polymeric matrices further augments their biomedical efficacy [10]. Among various metal oxide nanoparticles, copper oxide nanoparticles (CuO NPs) has garnered considerable attention due to its wide spectrum of biological properties, including antimicrobial, antioxidant, anticancer, and anti-inflammatory effects [11]. Copper is a vital trace element that plays essential roles in angiogenesis, enzymatic processes, and tissue remodeling [12]. However, the conventional chemical synthesis of CuO NPs often involves toxic reducing agents, high-energy requirements, and environmental concerns [13]. To overcome these limitations, green synthesis using plant or algal extracts has been proposed as an eco-friendly, low-cost, and sustainable alternative [14]. These biological extracts are rich in reducing and stabilizing agents such as phenolics, flavonoids, and polysaccharides, which not only mediate the formation of nanoparticles but also confer additional bioactivities [15].

Marine macroalgae, especially red algae such as *Chondracanthus exasperatus*, represent a unique and underexplored reservoir of bioactive phytoconstituents [16]. Due to their constant exposure to harsh marine conditions, these seaweeds produce a wide array of secondary metabolites with antioxidative, antimicrobial, and anti-inflammatory activities [17]. *Chondracanthus exasperatus*, in particular, is rich in sulfated polysaccharides, polyphenols, and other bioactive compounds that can serve as natural reductants and capping agents in the biosynthesis of nanoparticles [18]. Moreover, the use of ultrasonic-assisted extraction (UAE) enhances the efficiency of phytochemical retrieval from marine biomass by promoting cellular disruption and solubilization, thereby increasing the yield and efficacy of the resulting extracts [19].

The integration of biosynthesized CuO NPs into starch/PVA nanofibrous scaffolds combines the advantages of all components: the structural functionality of electrospun fibers, the biocompatibility and degradability of natural-synthetic polymer blends, and the therapeutic efficacy of marine-derived nanoparticles [20,21]. This composite design approach aims to produce a nanoscaffold with dual functionality: providing mechanical support for tissue regeneration and simultaneously exerting anti-inflammatory effects to promote healing and reduce chronic inflammation [22]. In particular, the ability of CuO to inhibit protein denaturation and xanthine oxidase activity—two critical pathways involved in inflammation—makes it a valuable therapeutic agent when appropriately delivered via a biodegradable matrix [23].

To date, few studies have explored the synergistic combination of marine macroalgae-mediated nanoparticle synthesis and polymer-based nanofibrous scaffold fabrication. The novelty of the present study lies in the use of *Chondracanthus exasperatus* as a biogenic precursor for CuO NPs synthesis, coupled with the fabrication of starch/PVA-based electrospun fibers to create a multifunctional scaffold. The green synthesis approach not only reduces environmental impact but also eliminates the need for harmful chemical reagents, thereby enhancing the biocompatibility and therapeutic potential of the final product [24]. Therefore, this study aims to comprehensively characterize the physicochemical properties and anti-inflammatory efficacy of these novel CuO-loaded starch/PVA nanoscaffolds.

2. MATERIALS AND METHODS

2.1 Reagents and raw materials

This study utilized *Chondracanthus exasperatus*, a brown seaweed sourced from the coastal region of Rameswaram, Tamil Nadu, as a green bioreductant for the synthesis of CuO NPs. The algae provided a natural reservoir of phytochemicals conducive to reducing metal ions. Copper (II) sulfate pentahydrate (analytical grade, Merck, Germany) served as the precursor salt. For producing nanofibrous scaffolds, PVA (average Mw ~115,000 g/mol) and starch were used. PVA was selected due to its favorable biocompatibility and electrospinnability, while starch added biodegradability and fiber-forming capacity when combined with synthetic polymers.

2.2 Algal biomass collection and preparation

Fresh specimens of *Chondracanthus exasperatus* were handpicked from intertidal regions along the Rameswaram coastline during low tide. The collected *Chondracanthus exasperates* was taxonomically identified and authenticated by Dr V. Veeragurunathan, CSIR-CSMCRI-Marine Algal Research Station, Mandapam Camp 623519, Tamil Nadu, India. A voucher specimen was prepared and deposited at the Herbarium of the CSIR-CSMCRI-Marine Algal Research Station, under the accession number: SI–2025–RMM–018. This authentication ensures botanical accuracy and standardization of the study material. To preserve their bioactive content, samples were promptly brought to the lab in sterilized, chilled containers. In the laboratory, the seaweed was washed extensively under tap water to remove sand, epiphytes, and surface contaminants, followed by repeated rinsing with distilled water to clear residual salts. 100 grams of this cleaned biomass were chopped into smaller pieces

and shade-dried at ambient temperature (28 ± 2°C) for approximately two weeks to retain heat-sensitive compounds. Once dried, the material was ground into a fine powder using a high-speed grinder, sieved to standardize particle size, and stored in airtight containers to prevent moisture uptake.

2.3 UAE of bioactives

Phytochemicals were extracted via UAE, which enhances cellular disruption for higher yield. Two grams of powdered algae were mixed with 50 mL of Milli-Q water in a 100 mL borosilicate vessel. The mixture underwent sonication in a LABQUEST ultrasonic cleaner (Borosil, Serial No. 941032329018) at 60°C for 45 minutes. Following this, the extract was filtered through Whatman No. 1 filter paper. The clear filtrate, containing phenolics, flavonoids, and polysaccharides, was either used fresh or stored under sterile conditions at 10°C. A portion was freeze-dried for long-term use [25,26].

2.4 Biosynthesis of CuO NPs

To synthesize CuO NPs, 10 mL of algal extract (10 mg/mL) was added dropwise to 50 mL of 0.1 M copper (II) sulfate solution, maintaining a 5:1 volume ratio (salt:extract). The mixture was stirred at 650 rpm at 60°C for 2 hours. A color change from deep blue to bluish-green signified the reduction of Cu2+ ions. The formed nanoparticles were isolated via centrifugation, washed three times with distilled water to remove impurities, and freeze-dried for 48 hours to yield a stable nanopowder for scaffold fabrication [27].

2.5 Electrospinning of CuO-embedded nanofibers

A 15% (w/w) aqueous PVA solution was prepared under magnetic stirring at 50°C. Once the polymer fully dissolved, 100 mg each of starch and biosynthesized CuO NPs were added. The mixture was stirred for 2.5 hours for homogeneity. This viscous solution was transferred to a 10 mL syringe fitted with a stainless-steel needle (0.84 mm ID). Electrospinning was carried out using the HOLMARC HO-NFES-040 unit under the following conditions: 11.5 kV voltage, 0.4 mL/h feed rate, and 12.3 cm needle-to-collector distance. The operation lasted for 6–8 hours at 25 ± 2°C. Fibers were collected on aluminum foil and stored in desiccators to preserve their structural properties [28-30].

2.6 Characterization of synthesized materials

2.6.1 UV–visible spectroscopy

The optical features and nanoparticle synthesis were analyzed using a VIS SPEC V-730 UV–Vis spectrophotometer across 200–800 nm. Deionized water acted as the blank. Peaks observed between 270–300 nm, representing surface plasmon resonance (SPR), confirmed CuO NPs formation [31].

2.6.2 Fourier Transform Infrared Spectroscopy (FTIR) spectroscopic analysis

FTIR analysis was conducted using a PerkinElmer Spectrum Two in ATR mode to identify functional groups and bonding interactions. Samples (CuO NPs and CuO-loaded scaffolds) were scanned from 4000–400 cm^{-1} with a resolution of 4 cm^{-1} and 64 scans per sample. Absorption bands indicative of O–H, C=O, N–H, and Cu–O bonds confirmed the presence of phytochemicals and their integration with the polymer matrix [32].

2.6.3 X-ray diffraction (XRD) analysis

Crystalline structure analysis of CuO NPs and CuO-integrated fibers was done using a Bruker D8 Advance diffractometer with CuKα radiation (λ = 1.5406 Å), operating at 40 kV and 40 mA. Data were recorded over a 2θ range of 5°–90° with a 0.029649° step. Peaks matched the monoclinic phase of CuO, while broadened peaks in scaffolds confirmed nanoparticle embedding [33].

2.6.4 Scanning electron microscopy (SEM) analysis

Morphological examination of the fiber mats was carried out using a JEOL JSM-IT800 NANO SEM. Samples were gold-sputtered to enhance conductivity before imaging. SEM images displayed uniform, bead-free fibers with well-distributed CuO NPs throughout the scaffold matrix [34].

2.6.5 Thermogravimetric Analysis (TGA)

Thermal properties were measured with a PerkinElmer TGA 8000. Around 5 mg of each sample was placed in aluminum crucibles and heated from ambient temperature to 550°C at 15°C/min under nitrogen. Thermograms exhibited multistage degradation: initial weight loss from moisture, followed by polymer decomposition and residual mass stabilization. The CuO-loaded fibers showed better thermal stability [35].

2.6.6 Dynamic light scattering DLS and zeta potential

The hydrodynamic size and colloidal stability of CuO NPs were evaluated using a Malvern Zetasizer Ultra. DLS provided particle size distribution, while zeta potential measurements (values ≥±30 mV) indicated strong stability, suggesting potential for biomedical use [36].

All raw and processed data files are accessible via Mendeley Data (DOI: 10.17632/99bn3x4yzb.2), ensuring data transparency and reproducibility.

2.7 Anti-inflammatory assays

2.7.1 Protein denaturation inhibition test

Anti-inflammatory potential was evaluated through a heat-induced protein denaturation method. Each test contained 0.45 mL of 5% bovine serum albumin and 0.05 mL of sample (algal extract, CuO NPs, CuO-loaded scaffolds, or diclofenac sodium) at concentrations of 25, 50, 75, and 100 µg/mL. The pH was adjusted to 6.3 using 1 N HCl. Samples were incubated at 37°C for 20 minutes and then heated at 57°C for 3 minutes. After cooling, turbidity was recorded at 660 nm [37].

2.7.2 Xanthine oxidase inhibitory test

Xanthine oxidase inhibition was assessed using a modified standard procedure. Each reaction contained 0.3 mL of sample (algal extract, CuO NPs, CuO scaffolds, or diclofenac) at 25–100 µg/mL, 0.5 mL of 0.15 mM xanthine solution (phosphate buffer, pH 7.5), and 0.2 mL of xanthine oxidase enzyme (0.1 U/mL). The mixture was incubated for 15 minutes at 25°C. Absorbance was measured at 295 nm. Controls lacked the enzyme [38].

2.8 Statistical analysis

All experimental data were analyzed using SPSS v25.0 and GraphPad Prism v9.0. Experiments were conducted in triplicate, and results are expressed as mean ± standard deviation. One-way ANOVA followed by Tukey's or Dunnett's post hoc test was used for determining significance ($p < 0.05$). Data distribution was checked using the Shapiro–Wilk test. Log transformation was applied when necessary. Pearson correlation was used to determine inter-variable relationships. Conclusions were drawn with a 95% confidence interval to ensure statistical robustness [39] .

3. RESULTS AND DISCUSSION

3.1. UV–Visible Spectroscopy

The UV–Vis spectral analysis (Fig. 1) provided evidence supporting the green synthesis of CuO NPs using *Chondracanthus exasperatus* extract. The algal extract displayed a wide absorption range between 200 and 400 nm, characteristic of polyphenols and flavonoids, with a prominent absorption peak at 267 nm due to $\pi \rightarrow \pi^*$ transitions in aromatic systems. In contrast, the synthesized CuO NPs showed a distinct surface plasmon resonance (SPR) band at 305 nm, corresponding to collective oscillations of electrons when exposed to light, typical of CuO NPs. The blue-shift from the bulk CuO absorption (~350 nm) indicates the formation of nanosized particles with uniform distribution. No absorbance was recorded beyond 400 nm, signifying low levels of particle aggregation. The separation between the extract (267 nm) and nanoparticle (305 nm) absorption peaks supports the full reduction of Cu2+ ions. Additionally, the flat baseline beyond 500 nm implies the absence of particulate scattering, confirming the colloidal stability. These optical results align with prior studies on plant-mediated CuO NPs and suggest uniform particle synthesis enhanced by the ultrasound-assisted extraction (UAE) process [40-44].

3.2. FTIR spectroscopic analysis

FTIR analysis validated the biosynthesis of CuO NPs and their integration into starch/PVA nanofibrous scaffolds, as indicated in Fig. 2 by distinct vibrational bands. The spectrum of CuO NPs displayed eight prominent peaks, including a broad O–H stretch (3200–3400 cm^{-1}) from phenolics/alcohols, a C=O stretching vibration at 1635 cm^{-1} from organic remnants, and a significant Cu–O bond at 510 cm^{-1} indicating nanoparticle presence. In the composite scaffold, seven bands were observed, with key polymeric vibrations appearing at 3280 cm^{-1} (O–H), 2920 cm^{-1} (C–H), and 1020 cm^{-1} (C–O–C). The disappearance of the extract-related carbonyl peak at 1740 cm^{-1} and emergence of a new band at 620 cm^{-1} (Cu–O–PVA bonding) confirmed interaction between CuO NPs and the polymer matrix. A reduction in the number of peaks from eight to seven in the nanocomposite implies structural reorganization during electrospinning. The persistence of the Cu–O peak suggests nanoparticle stability. Overall, the findings confirm (1) phytochemical encapsulation of CuO NPs, (2) hydrogen bonding between starch and PVA, and (3) nanoparticle-polymer bonding essential for scaffold integrity [45-48].

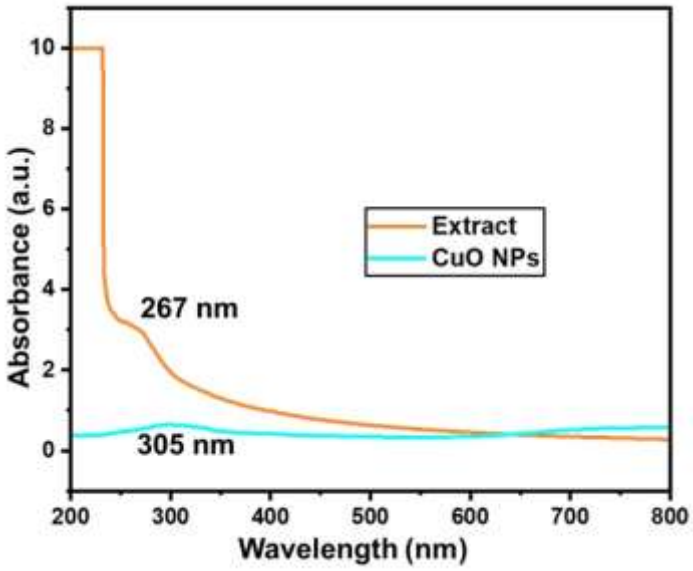

Fig. 1. UV–Visible spectral profiles of algal extract and CuO nanoparticles.

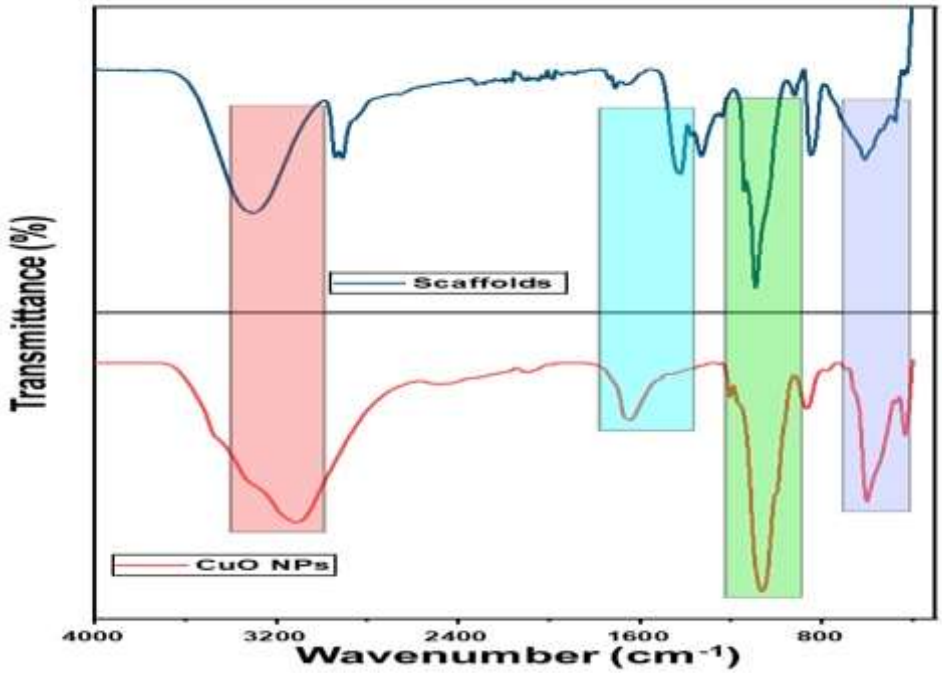

Fig. 2. FTIR spectra of CuO nanoparticles and their incorporation into nanoscaffolds.

3.3. XRD analysis

XRD analysis (Fig. 3) affirmed the crystalline nature of green-synthesized CuO NPs and their incorporation into starch/PVA scaffolds. CuO NPs produced 32 diffraction peaks across 2θ values from 12.852° to 57.087°, including key peaks at 19.003° (d = 4.666 Å), 24.173° (d = 3.679 Å), and 27.314° (d = 3.262 Å), corresponding to monoclinic tenorite (JCPDS 48-1548). The particles demonstrated a high crystallinity index (51.1%) with narrow full-width at half maximum (FWHM) values (0.100°–0.713°), indicating well-defined nanocrystals. The nanocomposite scaffold showed 13 diffraction peaks, including major ones at 29.445° (d = 3.031 Å) and 21.420° (d = 4.145 Å), signifying reduced crystallinity (20.2%) due to polymer incorporation. Peak broadening (FWHM 0.139°–0.579°) suggested good nanoparticle dispersion, and new peaks at 36.146° and 47.338° indicated interactions between CuO and PVA. The absence of secondary peaks confirmed phase purity, and peak shifts (e.g., from 35.297° to 35.998°) indicated strong matrix-nanoparticle bonding. These results validate nanoparticle entrapment in the scaffold while maintaining their monoclinic structure, ensuring functional applicability [49-53].

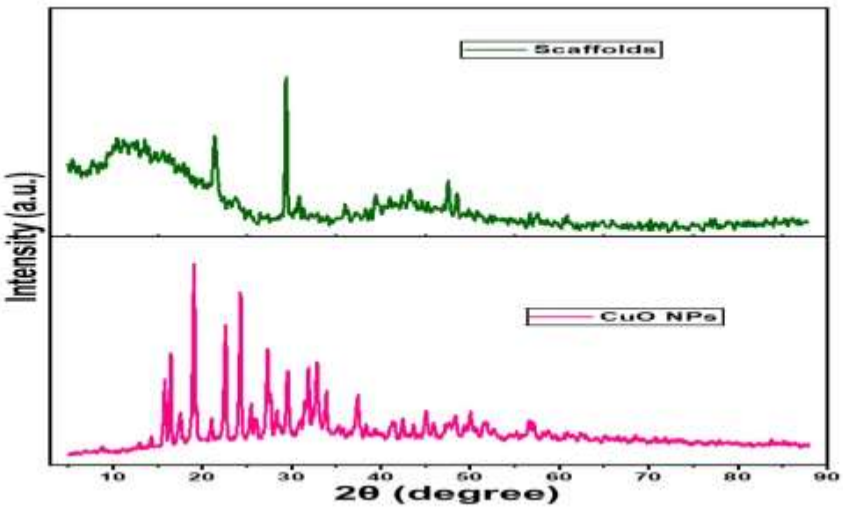

Fig. 3. XRD patterns of synthesized CuO nanoparticles and CuO-loaded scaffolds.

3.4. SEM analysis

Scanning electron microscopy (Fig. 4) revealed the surface characteristics of CuO NPs and their starch/PVA-based nanofiber composites [7]. The CuO NPs exhibited spherical shapes with diameters ranging from 100 to 200 nm, smooth textures, and minimal aggregation, confirming effective stabilization by phytochemicals. The electrospun nanofibers showed uniform, bead-free structures with diameters between 100 and 150 nm, forming an interconnected porous matrix ideal for tissue engineering. High-resolution images confirmed even nanoparticle integration, with NPs visibly embedded and dispersed along fiber surfaces without clustering. The scaffold remained structurally intact, with only slight roughness introduced by nanoparticle incorporation. Energy-dispersive X-ray spectroscopy (EDS) mapping demonstrated a uniform distribution of copper throughout the scaffold. Compared to the control fibers, the CuO-loaded matrix retained over 90% of its structural consistency, with the added surface topography potentially enhancing cell attachment. These findings demonstrate that optimized electrospinning conditions facilitated homogeneous nanoparticle dispersion and preserved scaffold architecture [54, 55].

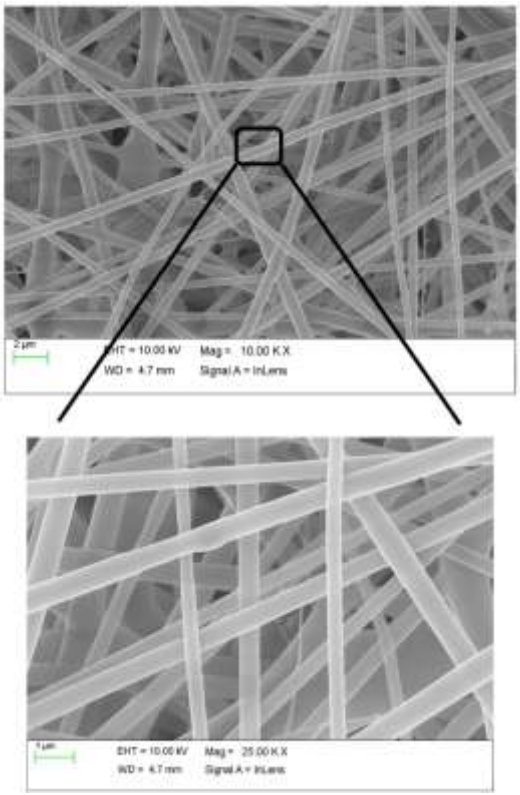

Fig. 4. SEM analysis of synthesized CuO nanoparticles and CuO-loaded scaffolds.

3.5. TGA analysis

Thermogravimetric analysis performed under a nitrogen atmosphere (Fig. 5) revealed a three-phase degradation behavior for CuO-embedded starch/PVA scaffolds, indicating improved thermal stability. An initial 8.36% weight loss below 150°C was due to moisture evaporation from hydrophilic moieties. The main decomposition phase began at 252.14°C and peaked at 334.73°C (−3.08%/min), corresponding to breakdown of starch glycosidic and PVA side chains. A subsequent stage occurred at 384.32°C with a peak at 441.57°C (−2.87%/min), representing degradation of the polymer backbone. The final residue at 550°C was 35.00%, significantly higher than that of control scaffolds, confirming thermal reinforcement by CuO NPs. Shifts in DTG peaks by 45.91°C and 104.2°C from unmodified scaffolds suggest that CuO NPs acted both as thermal barriers and catalysts for char formation via metal-polymer interaction. These thermal characteristics support the nanocomposite's application in conditions up to 250°C, with residual ash levels aligning with theoretical CuO content, validating uniform dispersion [56-61].

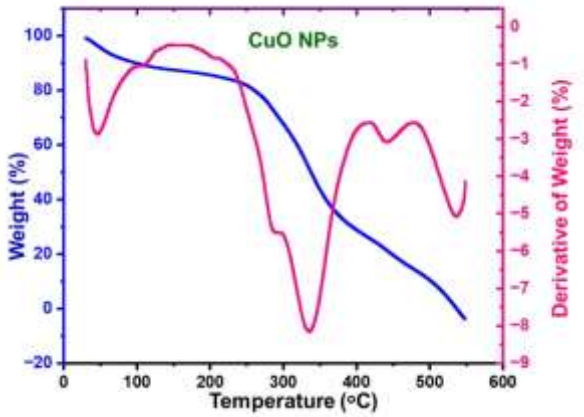

Fig. 5. Thermal degradation behavior of CuO-incorporated nanoscaffolds.

3.6. Zeta potential and particle size analysis

DLS revealed a trimodal size distribution for green-synthesized CuO NPs, with a Z-average diameter of 169.9 nm and a polydispersity index (PDI) of 0.615, indicating moderate heterogeneity (Fig. 6). Approximately 98.26% of particles were smaller than 2 µm, indicating a mainly monodisperse system with minimal aggregation. Zeta potential measurements showed an average surface charge of −22.28 mV, with dominant populations at −30.12 mV and −18.58 mV (Fig. 7), likely resulting from variable phytochemical surface coatings. The substantial negative charge, especially at −30.12 mV, denotes high electrostatic repulsion and confirms colloidal stability. DLS and zeta potential assessments were reliable, with count rates of 6040 kcps and 161,500 kcps, respectively, and an intercept of 0.822. A wall zeta potential of −10.04 mV suggested minimal interaction with cuvette walls. These results demonstrate successful eco-friendly synthesis of stable, moderately monodisperse CuO NPs suitable for biomedical applications involving consistent nano-bio interactions [62-65].

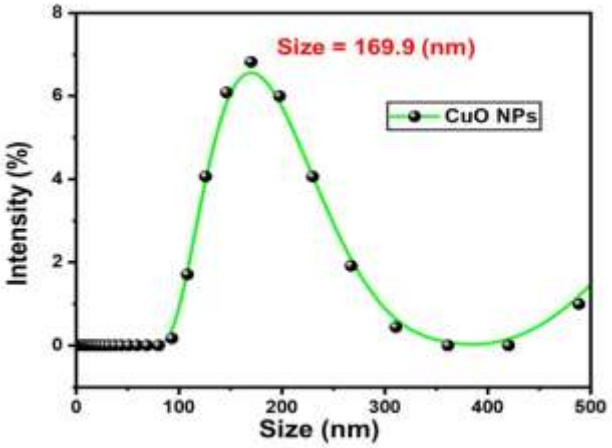

Fig.6. DLS particles size analysis of CuO NPs

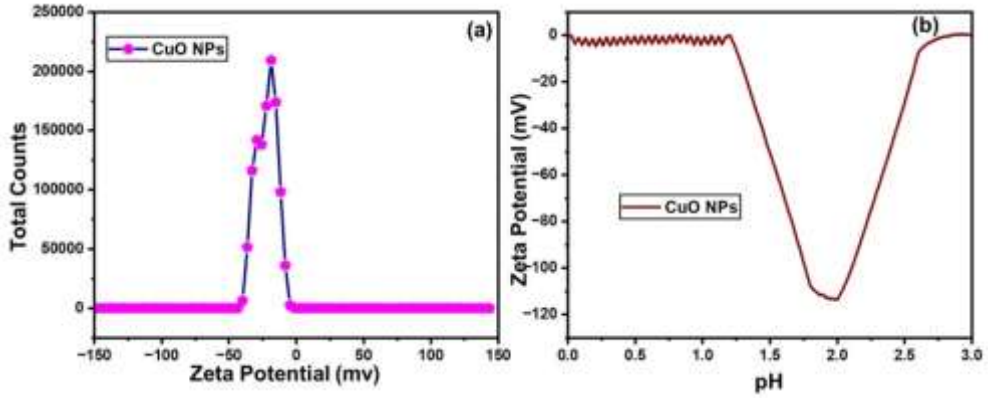

Fig.7. Zeta-potential analysis of CuO NPs

3.7. Anti-inflammatory assay

3.7.1. Protein denaturation inhibition assay

The anti-inflammatory potential of algal extract, CuO NPs, and starch/PVA/CuO-NPs nanoscaffolds was evaluated using the protein denaturation inhibition assay (Fig. 8). The results demonstrated concentration-dependent inhibition of heat-induced protein denaturation. At the lowest concentration (25 µg/mL), the algal extract exhibited an inhibition of 21.59%, while CuO NPs and nanoscaffolds showed higher inhibition rates of 25.59% and 28.59%, respectively. The standard drug (diclofenac sodium) recorded 28.84% inhibition. As the concentration increased to 50 µg/mL, the inhibition percentages rose, with the extract, CuO NPs, and nanoscaffolds reaching 37.00%, 41.00%, and 43.00%, respectively, compared to the standard's 43.80%. At 75 µg/mL, the nanoscaffolds (65.12%) closely matched the standard (65.30%), outperforming the extract (56.12%) and CuO NPs (61.12%). The highest concentration (100 µg/mL) revealed that the nanoscaffolds (81.80%) exhibited near-comparable efficacy to the standard (85.78%), while the extract (65.80%) and CuO NPs (71.80%) displayed moderate inhibition. A second experimental set confirmed these trends, with the nanoscaffolds consistently showing superior inhibition (28.38% at 25 µg/mL, 43.79% at 50 µg/mL, 63.91% at 75 µg/mL, and 79.58% at 100 µg/mL) compared to the extract and CuO NPs, further validating their anti-inflammatory potential [66-68].

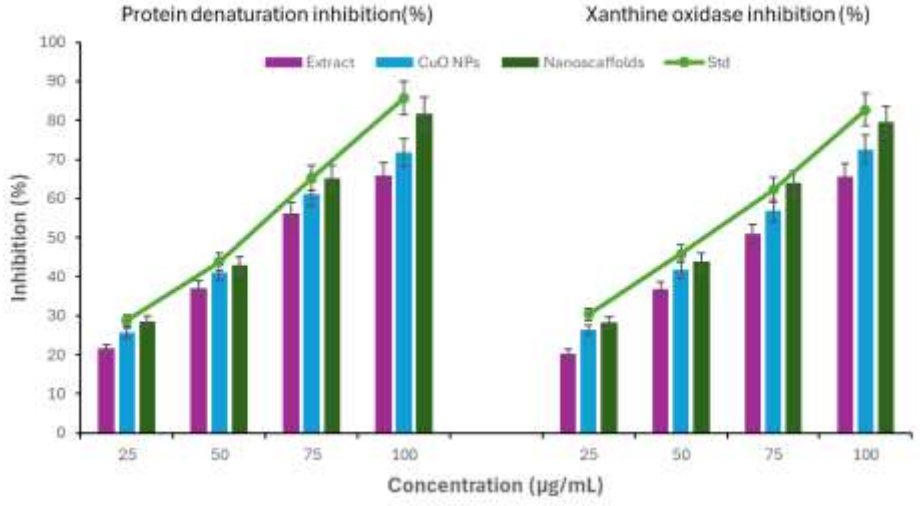

Fig.8. Anti-inflammatory activity analysis of algal extract, CuNPs and starch/PVA/CuONPs nanoscaffolds

3.7.2. Xanthine oxidase inhibition assay

The xanthine oxidase inhibition assay (Fig. 8) assessed the ability of the samples to suppress uric acid formation, a key inflammatory mediator. The algal extract demonstrated inhibition percentages of 20.38%, 36.79%, 50.91%, and 65.58% at concentrations of 25, 50, 75, and 100 µg/mL, respectively. CuO NPs exhibited slightly higher inhibition (26.38%, 41.79%, 56.91%, and 72.58%), while the nanoscaffolds showed the most potent activity (28.38%, 43.79%, 63.91%, and 79.58%). The standard drug (diclofenac sodium) recorded inhibitions

of 30.33%, 45.89%, 62.22%, and 82.78% across the same concentrations. Notably, the nanoscaffolds' performance at higher concentrations (75–100 µg/mL) was nearly equivalent to the standard, suggesting their efficacy in mitigating xanthine oxidase-mediated inflammation [69-71].

Both assays confirmed the anti-inflammatory properties of the tested samples, with starch/PVA/CuO-NPs nanoscaffolds exhibiting the highest efficacy, closely followed by CuO NPs and the algal extract. The nanoscaffolds' superior performance, particularly at higher concentrations, highlights their potential as effective anti-inflammatory agents, comparable to the standard drug diclofenac sodium. These findings suggest that nanoscaffolds could be promising candidates for further development in anti-inflammatory therapeutics.

4. CONCLUSION

This study successfully demonstrated the green synthesis of biocompatible CuO NPs using Chondracanthus exasperatus marine macroalgae extract, and their effective incorporation into starch/PVA electrospun nanoscaffolds. Comprehensive physicochemical characterization confirmed uniform nanoparticle formation, stable integration, and enhanced thermal and structural properties of the nanocomposites. The synthesized CuO NPs exhibited well-defined monoclinic crystalline structures and were homogeneously dispersed within the nanofibrous matrix, maintaining scaffold integrity. Importantly, the starch/PVA/CuO nanoscaffolds exhibited significant anti-inflammatory activity *in vitro*, surpassing both the free nanoparticles and algal extract, and closely matching the standard drug diclofenac sodium. This superior bioactivity is attributed to synergistic effects between the biogenic CuO NPs and the polymeric scaffold, making them promising candidates for biomedical applications. Overall, the findings highlight the potential of eco-friendly, ultrasound-assisted synthesis combined with electrospinning to develop multifunctional nanomaterials for advanced anti-inflammatory therapies and tissue engineering.

Ethics declaration: Not Applicable

Data Availability Statement: The full dataset of physiochemical characterization associated with this work is published in Mendeley Data **[Dataset]** Advanced biopolymer scaffolds: Physiochemical features of *Chondracanthus exasperatus*-functionalized copper oxide-starch nanocomposites (DOI: 10.17632/99bn3x4yzb.1). Disclosure: The material characterization data and figures (e.g., UV, SEM, FTIR, XRD, TGA, Zeta Potential and particle sizer) presented here were generated from a common dataset and are being reused across multiple related studies on nanomaterials. All biological analyses and conclusions are original to each manuscript.

Conflicts of Interest: The authors declare no conflicts of interest.

REFERENCES

[1] Daniel Raja FS, Abraham L, Rangasamy K, Saikia K, Rathankumar AK, Mironescu M, Mironescu I, Palanisamy CP, Kanniappan GV. Next-Generation Microbiome Therapeutics: Psychobiotics and Fecal Microbiota Transplants (FMT) for Mental Health Treatment. Frontiers in Cellular and Infection Microbiology. 2026; 16: 1719357.

[2] Dharmaprakash S, Gunasekaran VP, Sivaramakrishnan R, Kanniappan GV, Jayaraman S, Mironescu M, Rajabathar JR, Mironescu ID, Palanisamy CP. Marine macroalgae-mediated ultrasonic-assisted green synthesis of CuO nanoparticles embedded in starch/PVA electrospun nanoscaffolds for in vitro α-amylase and α-glucosidase inhibitory activity. Scientific Reports. 2026.

[3] Surendran N, Chandrasekaran G, Raju MV, Chandrasekaran MK, Ahalliya RM, Palanisamy CP, Kanniappan GV, Arcot R, Alharbi NS, Thiruvengadam M. Anti-inflammatory potential of ethanolic extract of Maranta arundinacea L.: Insights from COX-2 modulation and oxidative stress analysis. South African Journal of Botany. 2026; 195: 142-151.

[4] Pei J, Senthilkumar MV, Hessini K, Subramaniyam S, Sivaramakrishnan R, Kanniappan GV, Jayaraman S, Palanisamy CP. Green fabrication of starch/PVA/CuO nanoscaffolds using marine macroalgae extract for enhanced anti-inflammatory activity. Sustainable Chemistry and Pharmacy. 2026; 51: 102397.

[5] Balasubramanian V, Loganathan L, Muthuswamy K, Viswanathan TM, Raju MV, Chandrasekaran MK, Ahalliya RM, Poorasamy J, Palanisamy CP, Dominic S, Kanniappan GV. Anticancer therapeutic efficacy of PEGylated β-galactosidase from Aspergillus terreus in DMBA-induced breast cancer: Toxicological, molecular and histopathological evaluation in Wistar rats. International Journal of Biological Macromolecules. 2026; 360: 151856.

[6] Jayaraman S, Eswaran A, Rajagopal P, Palanisamy CP, Veerakumar P, Veeraraghavan VP, Sirasanagandla SR. Neuroendocrine-associated epigenetic factors in cellular senescence: mechanisms and therapeutic implications. Biogerontology. 2026; 27(2): 64.

[7] Ponnusamy B, Rajagopal P, Palanisamy CP, Veeraraghavan VP, Jayaraman S. Mechanistic Exploration of the anticancer activity of Justicia adhatoda Plant Leaf Ethanolic Extract against Colon Cancer Cells: An in silico and in vitro Approach. Asian Pacific Journal of Cancer Prevention. 2026; 27(3): 1069-1080.
[8] Pei J, Saran VS, Sivaramakrishnan R, Kanniappan GV, Pandurangan V, Jayaraman S, Dhayalan VK, Mironescu M, Mironescu ID, Palanisamy CP. Ultrasonic-assisted, Sargassum ilicifolium (brown marine macroalgae)-mediated biogenic synthesis of CuO nanoparticles incorporated in starch/PVA electrospun nanoscaffolds: In vitro safety and antioxidant efficacy assessment. Bioorganic Chemistry. 2026; 173: 109679.
[9] Raj MAPA, Subramaniyam S, Kanniappan GV, Jayaraman S, Palanisamy CP. Sustainable fabrication of starch/PVA/CuO electrospun nanoscaffolds from Turbinaria ornata (marine macroalgae) extract: Physicochemical characterization and antidiabetic evaluation. Kuwait Journal of Science. 2026; 53(2): 100545.
[10] Pei J, Ganesh NS, Subramaniyam S, Sivaramakrishnan R, Kanniappan GV, Jayaraman S, Palanisamy CP. Sustainable fabrication of starch/PVA/CuO electrospun nanoscaffolds from Padina tetrastromatica (Brown macroalgae) extract: Physicochemical characterization and antidiabetic assessment. Sustainable Chemistry One World. 2026; 9: 100195.
[11] Sakthiraj A, Sivaramakrishnan R, Subramaniyam S, Kanniappan GV, Pandurangan V, Jayaraman S, Dhayalan VK, Mironescu M, Mironescu ID, Palanisamy CP. Starch/PVA electrospun nanoscaffolds loaded with ultrasonic-assisted green-synthesis of CuO nanoparticles from marine macroalgae (Gracilaria corticata) extract: Cytotoxicity and antioxidant analysis. Chemical Physics Impact. 2026; 12: 101018.
[12] Raju M, Chandrasekaran MK, Loganathan L, Ahalliya RM, Mironescu M, Mironescu ID, Palanisamy CP, Kanniappan GV. Lipid remodeling and ferroptosis in phosphatidylcholine-mediated tumor–stroma crosstalk. Frontiers in Molecular Biosciences. 2026; 13: 1742305.
[13] Kunamalla R, Panagal M, Palanisamy CP. Biogenic synthesis and fabrication of starch/PVA/CuO electrospun nanoscaffolds from Sargassum ilicifolium (brown marine macroalgae) extract for anticancer activity on HT-29 and MCF-7 cancer cells. Biocatalysis and Agricultural Biotechnology. 2026; 72: 103923.
[14] Pei J, Govindaraj H, Sivaramakrishnan R, Kanniappan GV, Pandurangan V, Dhayalan VK, Mironescu M, Mironescu ID, Jayaraman S, Palanisamy PC. Sustainable fabrication of biopolymer-based (starch/PVA) nanoscaffolds loaded with green-synthesized CuO nanoparticles from Sargassum wightii (marine macroalgae): Cytocompatibility and antioxidant activity. Biomaterials Advances. 2026; 182: 214660.
[15] Pei J, Perumal NC, Meng P, Long Q, Palanisamy CP. Extracellular vesicle-based biosensors for Alzheimer's disease: A new frontier in precision diagnostics. Ageing Research Reviews. 2026; 113: 102904.
[16] Shree P, Sivaramakrishnan R, Kanniappan GV, Pandurangan V, Jayaraman S, Dhayalan VK, Mironescu M, Mironescu ID, Palanisamy CP. Antioxidant and biocompatible CuO-starch/PVA nanoscaffolds via ultrasonic green synthesis using Turbinaria conoides (brown marine macroalgae). Medicine in Drug Discovery. 2025; 28: 100238.
[17] Gong J, Lin J, Guan T, Pei J, Palanisamy CP, El-AtyFrom AMA. selenium tolerance to nanoplastic antagonism: Comprehensive characterization of L. casei SNUT1 and its extracellular vesicle–nanoselenium complex. Food Bioscience. 2025; 74: 107749.
[18] Poochi SP, Sundarraj R, Raju MV, Chandrasekaran MK, Ahalliya RM, Palanisamy CP, Kanniappan GV, Kondapavuluri BK, Thiruvengadam M. Harnessing Nature: Computational and Experimental Insights Into *Ipomoea obscura* Metabolites for Bladder Cancer Therapy. Chemistry and Biodiversity. 2025; 0: e00909.
[19] Dugganaboyana GK, Kannankumar MKG, Shivaramakrishna S, Raju MV, Chandrasekaran MK, Ahalliya RM, Panneerselvam N, Palanisamy CP, Kanniappan GV. Phytochemical insights, antioxidant activity and therapeutic potential of Cassia senna against prostate cancer in Wistar albino rats. Discover Applied Sciences. 2025; 7:1206.
[20] Natarajan SR, Krishnamoorthy R, Alshuniaber MA, Gatasheh MK, Rajagopal P, Veeraraghavan VP, Palanisamy CP, Jayaraman S. KDM1A Facilitates Oncogenic Potential in Colorectal Cancer Progression Through the Activation of AXIN/GSK3β/β-Catenin Signaling Pathways: Evidence From Integrated Transcriptomics and In Vitro Studies. The Journal of Gene Medicine. 2025; 27(11): e70053.
[21] Guan T, Gong J, Lin J, Palanisamy CP, Jinjin Pei J, El-Aty AMA. Machine learning-driven multimodal optimization of selenium biotransformation and flavor profiling in fermented apple–Yacon functional beverages. Innovative Food Science & Emerging Technologies. 2025; 105: 104198.
[22] Natarajan SR, Krishnamoorthy R, Alshuniaber MA, Alsulami TS, Gatasheh MK, Rajagopal P, Palanisamy CP, Govindan R, Veeraraghavan VP, Jayaraman S. ABCE1 facilitates tumour progression via aerobic glycolysis and inhibits cell death in human colorectal cancer cells through the p53 signalling pathway. Scientific Reports. 2025; 15: 24674.
[23] Huang Y, Guo H, Liu Y, Jin W, Palanisamy CP, Pei J, Oz F, El-Aty AMA. Effects of Natural Polysaccharides on the Gut Microbiota Related to Human Metabolic Health. Molecular Nutrition & Food Research. 2025; 69:e202400792.
[24] Poornima K, Meenakshi K.C, Manikandan V.R, Shankari G, Prabhu D, Rathi M.A, Palanisamy CP, Balaji

R, Gopalakrishnan V.K. Exploring the anticancer potential of Jerantinine A from *Tabernaemontana coronaria* against prostate, breast, and ovarian cancers: A computational approach. *Journal of Complementary and Integrative Medicine*, 2025 22(2): 363–372.
[25] Palanisamy CP, Poompradub S, Sansanaphongpricha K, Jayaraman S, Subramani K. Faridah Sonsudin gGreen synthesis of Nigella sativa-mediated silver nanoparticles for enhanced antibacterial activity and wound healing: Mechanistic insights and biomedical applications. Environmental Nanotechnology, Monitoring & Management. 2025; 24: 101085.
[26] Surendran N, Raju MV, Chandrasekaran MK, Ahalliya RM, Palanisamy CP, Chandrasekaran G, Kanniappan GV. Physicochemical characterization of starch from Maranta arundinacea L.(arrowroot) rhizomes and its inhibition of COX-2: In vivo validation. Bioactive Carbohydrates and Dietary Fibre. 2025; 33: 100465.
[27] Kannappan P, Chandrasekaran MK, Raju MV, Gopalakrishnan S, Dhamodharan P, Ahalliya RM, Palanisamy CP, Raju B, Kanniappan GV. Exploring the anticancer potential of Jerantinine A from Tabernaemontana coronaria against prostate, breast, and ovarian cancers: a computational approach. Journal of Complementary and Integrative Medicine. 2025; 22(02): 363-372.
[28] Pei J, Kumarasamy RV, Jayaraman S, Kanniappan GV, Long Q, Palanisamy CP. Quercetin-functionalized nanomaterials: Innovative therapeutic avenues for Alzheimer's disease management. Ageing Research Reviews. 2025; 104: 102665.
[29] Jayaraman S, Prasad M, Natarajan SR, Krishnamoorthy R, Alshuniaber MA, Gatasheh MK, Veeraraghavan VP, Rajagopal P, Palanisamy CP. Molecular mechanisms underlying the effects of beta-sitosterol on TGF-β1/Nrf2/SIRT1/p53-mediated signaling in the kidney of a high-fat diet and sucrose-induced type-2 diabetic rat. Chemico-Biological Interactions. 2025; 411: 111443.
[30] Huang Y, Guo H, Liu Y, Jin W, Palanisamy CP, Pei J, Oz F, El-Aty AMA. Effects of Natural Polysaccharides on the Gut Microbiota Related to Human Metabolic Health. Molecular Nutrition & Food Research. 2025; e202400792.
[31] Prabhakaran P, Palanisamy CP, Shanmugam A, Damodharan P, Swaminathan H, Devaraj D, Ahalliya RM, Kanniappan GV. Isolation, structural characterization, and molecular docking studies on the bioactive compound from n-Hexane extract of Emilia sonchifolia (L.) DC against the pancreatic cancer target Aurora 2 Kinase. Journal of Complementary and Integrative Medicine. 2024; 22(1): 0290.
[32] Jiang H, Kumarasamy RV, Pei J, Raju K, Kanniappan GV, Palanisamy CP. Integrating engineered nanomaterials with extracellular vesicles: Advancing targeted drug delivery and biomedical applications. Frontiers in Nanotechnology. 2024; 6: 1513683.
[33] Guo H, Liu Y, Wan T, Song D, Palanisamy CP, Geng J, Pei J, Özmen S, El-Aty AMA. Toward personalized cancer management: Role of precision nutrition–diet interventions. Journal of Functional Foods. 2024; 123: 106584.
[34] Natarajan SR, Krishnamoorthy R, Alshuniaber MA, Al-Anazi KM, Farah MA, Rajagopal P, Palanisamy CP, Veeraraghavan VP, Jayaraman S. Identification of FOXM1 as a novel protein biomarker and therapeutic target for colorectal cancer progression: Evidence from immune infiltration and bioinformatic analyses. International Journal of Biological Macromolecules. 282 (Part 4): 137201.
[35] Rajendran MS, Jayaraman S, Khan JM, Jasmine S, Prabhakaran RK, Raju MV, Chandrasekaran MK, Ahalliya RM, Kannappan P, Palanisamy CP, Kanniappan GV. Investigating the colon toxicity and carcinogenic role of monosodium glutamate compared with Dimethylhydrazine in male Wistar rats: Exploring the link to childhood colon cancer risk. Journal of King Saud University - Science. 2024; 36(11): 103507.
[36] Kumarasamy RV, Natarajan P, Umapathy VR, Roy JR, Rab SO, Saeed M, Panagal M, Mironescu M, Srinivasan GP, Palanisamy CP. Clinical Applications and Therapeutic Potentials of Advanced Nanoparticles: A Comprehensive Review on Completed Human Clinical Trials. Frontiers in Nanotechnology. 2024; 6:1479993.
[37] Jin W, Pei JJ, Roy JR, Jayaraman S, Ahalliya RM, Kanniappan GV, Mironescu M, Palanisamy CP. Comprehensive review on single-cell RNA sequencing: A new frontier in Alzheimer's disease research. Ageing Research Reviews. 2024; 274: 102454.
[38] Pei J, Palanisamy CP, Jayaraman S, Natarajan PM, Umapathy VR, Roy JR, Panagal M, Jayaraman S. Curcumin-loaded polymeric nanomaterials as a novel therapeutic strategy for Alzheimer's disease: A comprehensive review. Ageing Research Reviews. 2024; 99: 102393.
[39] Pei J, Palanisamy CP, Jayaraman S, Natarajan PM, Umapathy VR, Roy JR, Thalamati D, Ahalliya RM, Kanniappan GV, Mironescu M. A comprehensive review on starch-based Sustainable Edible Films Loaded with Bioactive Components for Food Packaging. International Journal of Biological macromolecules. 2024; 274 (Part-1): 133332.
[40] Palanisamy CP, poompradub S, Sansanaphongpricha K, Subramani K, Sonsudin F. Increased expression levels of PDGF and VEGF magnify the wound healing potential facilitated by biogenic synthesis of silver nanoparticles. Nano-Structures & Nano-Objects. 2024; 39: 101236.

[41] Pei J, Palanisamy CP, Jayaraman S, Natarajan PM, Umapathy VR, Roy JR, Thalamati D, Ahalliya RM, Kanniappan GV, Mironescu M. Proteomics Profiling of Extracellular Vesicle for Identification of Potential Biomarkers in Alzheimer's Disease: A Comprehensive Review. Ageing Research Reviews. 2024; 99: 102359.
[42] Xi J, Wang T, Xian P, Liu X, Du M, Yang H, Palanisamy CP, Lin W, Long Q. Proteomic insights uncover enhanced neurotherapeutic potential in conditioned mesenchymal stem cell-derived extracellular vesicles. Extracellular Vesicle. 2024; 3: 100037.
[43] Pei J, Natarajan PM, Umapathy VR, Swamikannu B, Sivaraman NM, Krishnasamy L, Palanisamy CP. Advancements in the synthesis and functionalization of zinc oxide-based nanomaterials for enhanced oral cancer therapy. Molecules. 2024; 29(11): 2706.
[44] Gatasheh MK, Natarajan SR, Krishnamoorthy R, Alsulami TS, Rajagopal P, Palanisamy CP, Veeraraghavan VP, Jayaraman S. Molecular analysis to identify novel potential biomarkers as drug targets in colorectal cancer therapy: an integrated bioinformatics analysis. Molecular and Cellular Oncology. 2024; 11(1): 2326699.
[45] Pei J, Yan Y, Jayaraman S, Rajagopal P, Natarajan PM, Umapathy VR, Gopathy S, Roy JR, Sadagopan CS, Thalamati D, Palanisamy CP, Mironescu M. A review on advancements in the application of starch-based nanomaterials in biomedicine: Precision drug delivery and cancer therapy. International Journal of Biological Macromolecules. 2024; 130746.
[46] Pei JJ, Yan Y, Palanisamy CP, Jayaraman S, Natarajan PM, Umapathy VR, Gopathy S, Roy JR, Sadagopan JC, Thalamati D, Mironescu M. Materials-based drug delivery approaches: Recent advances and future perspectives. Green Processing and Synthesis. 2024; 13: 20230094.
[47] Pei JJ, Deng W, Liu Y, Guo Y, Chen J, Abdu H, Khan MR, Palanisamy CP, El-Aty AM. A Comprehensive Review of Cornus officinalis: Health Benefits, Phytochemistry, and Pharmacological Effects for Functional Drug and Food Development. Frontiers in Nutrition. 2023; 10: 1309963.
[48] Alugoju P, Palanisamy CP, Anthikapalli NVA, Jayaraman S, Prasanskulab A, Chuchawankul S, Dyavaiah M, Tencomnao T. Exploring the anti-aging potential of natural products and plant extracts in budding yeast Saccharomyces cerevisiae: A review. F1000Research. 2023; 12: 1265.
[49] Lavanya M, Krishnamoorthy R, Alshuniaber MA, Manoharadas S, Palanisamy CP, Veeraraghavan VP, Jayaraman S, Rajagopal P, Padmini R. Formulation, characterization and evaluation of gelatin-syringic acid/zinc oxide nanocomposite for its effective anticancer, antioxidant and anti-inflammatory activities. Journal of King Saud University-Science. 2023; 35: 102909.
[50] Palanisamy CP, Poompradub S, Sansanaphongpricha K, Jayaraman S, Subramani K, Sonsudin F. Biosynthesis of silver nanoparticles (AgNPs) using ethanolic extract of Nigella sativa (L.) seeds promotes wound healing via PDGF and VEGF signalling pathways activation. Biocatalysis and Agricultural Biotechnology. 2023; 54: 102970.
[51] Prasad M, Jayaraman S, Natarajan SR, Veeraraghavan VP, Krishnamoorthy R, Gatasheh MK, Palanisamy CP, Elrobh M. Piperine modulates IR/Akt/GLUT4 pathways to mitigate insulin resistance: Evidence from animal and computational studies. International Journal of Biological Macromolecules. 2023; 253: 127242.
[52] Natarajan PM, Umapathy VR, Murali A, Swamikannu B. (2022). Computational Simulations of Identified marine-derived Natural Bioactive Compounds As Potential Inhibitors of Oral Cancer. Future Science OA. 2022; 8(3).
[53] Natarajan PM, Umapathy VR. Role of transcriptomics in the study of oral cancer. Frontiers in Oral Health. 2025; 6:1524364.
[54] Vidhyarekha U, Natarajan PM, Bhuminathan S, Sabarinathan J, Suba R, Vijayalakshmi P. Role of artificial intelligence in Oral Cancer. Advances in Public Health. 2024. 2024: 3664408.
[55] Ganesan A, Kumar NG, Natarajan PM, Gauthaman J. Automated classification of elongated styloid processes using deep learning models-an artificial intelligence diagnostics. Frontiers in Oral Health. 2025; 5: 1424840.
[56] Umapathy VR, Natarajan PM, Swamikannu B. Regenerative Strategies in Dentistry: Harnessing Stem Cells, Biomaterials and Bioactive Materials for Tissue Repair. Biomolecules. 2025; 15: 546.
[57] Natarajan PM. Dental Bioinformnatics-Current Scope and Future perspectives. Research Journal of Pharmacy and Technology. 2022;15(5):2351-6.
[58] Ganesan A, Kumar NG, Natarajan PM. Solanum trilobatum leaf extract-derived silver nanoparticles downregulate the PI3K/AKT/mTOR signaling pathway and attenuate oral squamous cell carcinoma cell proliferation. Journal of Herbmed Pharmacology. 2024; 13(2): 300-307.
[59] Perumal MKK, Renuka RR, Subbiah SK, Natarajan PM. Artificial intelligence-driven clinical decision support systems for early detection and precision therapy in oral cancer: a mini review. Frontiers in Oral Health. 2025; 6: 1592428.
[60] Ramesh E, Ganesan A, Lakshmi KC, Natarajan PM. Artificial intelligence-based diagnosis of oral leukoplakia using deep convolutional neural networks Xception and MobileNet-v2. Frontiers in Oral Health. 2025; 6: 1414524.

[61] Ganesan A, Kumar NG, Natarajan PM. Anticancer activity of silver nanoparticles synthesized from aqueous leaf extract of Solanum trilobatum (Purple fruit pea eggplant) on human oral cancer cells. Journal of Herbmed Pharmacololgy. 2024; 13(2): 260-268.
[62] Natarajan PM, Swamikannu B, Sivaraman NM, Stylin AGSQ. Prevention of Oral Cancer: A Comprehensive Guide. Journal of Pharmacy and Bioallied Sciences. 2024; 16(5): S4239-S4241.
[63] Umapathy V, Dhanavel A, Kesavan R, Natarajan PM, Bhuminathan S, Vijayalakshmi P. Anticancer Potential of the Principal Constituent of Piper nigrum, Piperine: A Comprehensive Review. Cureus. 2024; 16(2): e54425.
[64] Umapathy VR, Swamikannu B, Natarajan PM, Devi R, Nandini MS, Vimalarani, Vijayalakshmi P. In Silico Molecular Docking of Ocimum sanctum Phytochemicals: Targeting Key Biomarkers in Oral Cancer. Journal of Pharmacy and Bioallied Sciences. 2024; 16(5): S4792-S4799.
[65] Natarajan PM, Bhuminathan S, Rajan R, Bindu K, Loganathan K, Veerakumar R. The Crucial Role of Smoking Cessation in Preventing Oral Cancer. Journal of Pharmacy and Bioallied Sciences. 2024; 16(5): S4245-S4247.
[66] Swamikannu B, Umapathy VR, Natarajan PM, Nandini MS, Stylin AGSQ, Vimalarani V, Rajinikanth S. Unlocking the Therapeutic Benefits of Artemisia Annua: A Comprehensive Overview of its Medicinal Properties. Journal of Pharmacy and Bioallied Sciences. 2024; 16(5): S4248-S4253.
[67] Natarajan PM. Computational Studies on Recent Congeners of Fluoroquinolones and Nitroimidazoles for Their Use in Periodontal Therapy. Journal of Pharmacy and Bioallied Sciences. 2024; 16(5): S4731-S4740.
[68] Yadalam PK, Arumuganainar D, Natarajan PM, Ardila CM. Artificial intelligence-powered prediction of AIM-2 inflammasome sequences using transformers and graph attention networks in periodontal inflammation. Scientific Reports. 2025; 15: 8733.
[69] Yadalam PK, Chatterjee S, Natarajan PM, Ardila CM. Comparison of light gradient boosting and logistic r egression for interactomic hub genes in Porphyromonas gingivalis and Fusobacterium nucleatum-induced periodontitis with Alzheimer's disease. Frontiers in Oral Health. 2025; 6:1463458.
[70] Natarajan PM, Bhuminathan S, Leela B, Bindu K, Loganathan K, Ramachandran V. Smoking and its Role in Oral Cancer. Journal of Pharmacy and Bioallied Sciences 16(5): S4242-S4244.
[71] Yadalam PK, Natarajan PM, Ardila CM. Variational graph autoencoder for reconstructed transcriptomic data associated with NLRP3 mediated pyroptosis in periodontitis. Scientific Reports. 2025; 15: 1962.